Vortex properties of two-dimensional superconducting Pb films

2010 J. Phys.: Condens. Matter 22 065701

(http://iopscience.iop.org/0953-8984/22/6/065701)

J. Phys.: Condens. Matter **22** (2010) 065701 (5pp) doi:10.1088/0953-8984/22/6/065701

Vortex properties of two-dimensional superconducting Pb films

Y X Ning[1], C L Song[1,2], Y L Wang[1], Xi Chen[2], J F Jia[2], Q K Xue[1,2] and X C Ma[1]

[1] Institute of Physics, The Chinese Academy of Sciences, Beijing 100190, People's Republic of China
[2] Department of Physics, Tsinghua University, Beijing 100084, People's Republic of China

E-mail: xcma@aphy.iphy.ac.cn

Received 18 October 2009, in final form 24 December 2009
Published 21 January 2010
Online at stacks.iop.org/JPhysCM/22/065701

Abstract
Using low temperature scanning tunnelling microscopy/spectroscopy (STM/STS) we have investigated the vortex behaviours of two-dimensional superconducting Pb films at different thicknesses. STS at the vortex core shows an evolution of electronic states with film thickness. Transition from the clean limit to the dirty limit of superconductivity is identified, which can be ascribed to the decreased electronic mean free path induced by stronger scattering from the disordered interface at smaller thicknesses. A magnetic field dependent vortex core size is observed even for such a low-κ superconductor. The weak pinning induced by surface defects leads to the formation of a distorted hexagonal vortex lattice.

(Some figures in this article are in colour only in the electronic version)

1. Introduction

The vortex lattice in type-II superconductors was described by Abrikosov in 1957 [1]. Since then, many techniques such as neutron scattering [2], Bitter decoration [3], scanning tunnelling microscopy/spectroscopy (STM/STS) [4] and scanning Hall probe microscopy [5] have been used to study the properties of vortices. STM/STS is a powerful probe for detecting vortex structure due to its atomic-scale spatial resolution in real space. By measuring spatial variations of the local density of states (LDOS) on a superconductor surface with STS one can directly image individual vortex structures as well as the electronic states within the vortex cores. This technique has been used to image the vortex lattices of various compound superconductors, such as 2H-$NbSe_2$ [4, 6], MgB_2 [7] and Bi_2Sr_2CaCuO [8], as well as some amorphous transition-metal superconducting thin films [9, 10], revealing many interesting properties [11].

However, little work on elemental type-II superconductors has been reported, mainly due to their low superconducting transition temperature (T_c) and difficulty in preparing high quality film with well-controlled morphology. From this point of view, Pb film is a good choice because of its relatively high T_c [12] and easy preparation of an atomically flat surface [13–15]. Bulk lead is a type-I superconductor, and it transforms into type-II at a critical thickness of ~250 nm [16]. A corresponding transition from an intermediate state to a mixed state of the magnetic flux quanta was observed by the Bitter pattern [16] and electron-holography techniques [17].

Very recently, the vortex behaviours of nano-sized thin Pb islands have been investigated [18, 19] and the vortex lattice evolution with magnetic field was revealed [20] by STS. The former studies focused on a strong vortex confinement regime by using Pb island with a lateral size of 50–150 nm. The latter was performed on larger islands and revealed surface superconductivity at the periphery of the islands. No studies have been conducted on a uniform Pb film of micrometre size, which can be regarded as an infinite two-dimensional (2D) superconductor without many boundary effects. Also, little attention has been paid in previous works to the thickness related properties. In this paper, we report a low temperature STM/STS study of the vortex properties of atomically flat superconducting Pb films with different thicknesses. The high quality of the films allows us to investigate the thickness dependence of electronic states in the vortex cores, the magnetic field dependence of vortex core size and spatial distribution of vortices in a well-controlled way.

2. Experiment

The experiments were carried out on a Unisoku ultrahigh vacuum (UHV) low temperature (LT) STM system, which is

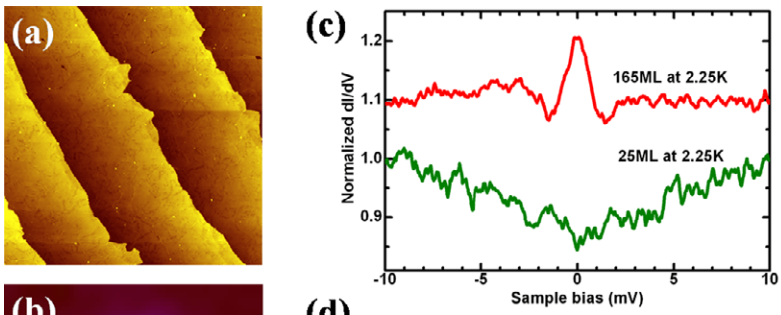

(d)

	ξ_0(nm)	$\xi_{GL}^{2.25K}$(nm)	l(nm)[a]	l(nm)[b]
25 ML	88.3	48.0	14.3	24.1
60 ML	84.7	69.4	34.3	38.7
165 ML	83.4	53.8	94.4	–

[a] Reference 15.
[b] Calculation for a dirty sample.

Figure 1. (a) STM image (1000 nm × 1000 nm) of an atomically flat Pb thin film of 25 ML. The image was taken with a sample bias $V_{\text{sample}} = 3.0$ V and a tunnelling current $I_t = 0.2$ nA. (b) Vortex image (468 nm × 468 nm) obtained from the 25 ML film under a magnetic field of 75 G at 2.25 K. The data were taken with a bias modulation 0.2 mV_{rms} at a frequency of 2 kHz. The tunnelling gap was set at $V_{\text{sample}} = 10$ mV and $I_t = 0.2$ nA. The bias was ramped to 0 V with feedback off at each pixel to record the ZBC. (c) $\text{d}I/\text{d}V$ spectra taken at the centre of the vortex core for different thicknesses at 75 G. The spectra are normalized to the differential conductance at high bias (±12 meV). The red curve is shifted by 0.1 for clarity. (d) Various results obtained using different methods (see the text).

equipped with a molecular-beam-epitaxy (MBE) chamber for *in situ* preparation of thin film samples. The substrate for growing Pb films is a p-type Si(111) wafer with a resistivity of 0.02 Ω cm and a miscut angle of 0.1° towards the $[11\bar{2}]$ direction. Clean Si(111)-7 × 7 surfaces were obtained using the standard procedure at a base pressure of 2×10^{-10} Torr [21]. The uniform Pb(111) thin films with an average terrace width of 180 nm were formed by depositing high-purity (99.999%) Pb from a Knudsen cell onto the clean Si(111)-7 × 7 surfaces held at 100 K followed by annealing at room temperature (RT) [12]. After growth, the samples were transferred to the LT-STM chamber which was maintained at 4.32 K by liquid helium cooling or 2.25 K by further pumping. A magnetic field up to 7 T can be applied perpendicular to the sample surface if needed. All STM measurements were performed in the constant current mode by using PtIr tips. STS was obtained using the standard lock-in technique with a small ac modulation of 0.2 mV at a frequency of 2 kHz, while the tunnel gap was kept at 10 mV/0.2 nA. The vortex imaging is based on the variation of LDOS inside and outside of a vortex in the presence of a magnetic field. A detailed description of the measurement has been reported elsewhere [20].

3. Results and discussion

3.1. Transition from the clean limit to the dirty limit

The first STM observation of the Abrikosov vortex lattice was achieved on a conventional superconductor, 2H-$NbSe_2$, by Hess *et al* [4]. An unexpected zero-bias conductance peak (ZBCP) was revealed at the centre of the vortex, which was assigned to low-energy quasiparticle bound states by subsequent theoretical studies [22, 23]. Later on, experimental observation of ZBCP as a function of disorder in an alloy system $Nb_{1-x}Ta_xSe_2$ showed that the conductance peak was only a property of the superconductor in the clean limit, while in the dirty limit the LDOS at the vortex core centre was exactly the same as that in the normal state [6]. In fact, for Pb films grown on an Si substrate, due to the interface scattering, a thickness induced transition from the clean limit to the dirty limit also exists.

Here we study the ZBC in the centre of a vortex on Pb films at different thicknesses. Figure 1(a) shows a typical topographic image of an atomically flat film over a macroscopic area. The thickness of the film is 25 monolayers (ML). The average terrace width is ∼180 nm, much larger than the BCS coherence length ($\xi_0 = 83$ nm) of bulk Pb. Under a magnetic field, the superconductivity is suppressed in the vortex core, leading to a drastic increase of LDOS at the Fermi surface (i.e. zero-bias conductance) which can be detected by STS [20]. The vortex formed in a 75 G magnetic field at 2.25 K is displayed in figure 1(b). The gapless normal state regions inside the vortex core are shown by a yellow colour (ZBC = 0.9) while the superconducting regions of low conductance are maroon-coloured (ZBC = 0.0).

The normalized differential conductance spectra at the vortex core for 25 ML (green curve) and 165 ML (red curve) Pb films are shown in figure 1(c). For the 25 ML film, the spectrum does not show any defined peak, as in the normal state (0 G, 10 K) [20, 24]. This dip feature of the $\text{d}I/\text{d}V$ spectrum at the normal state gives a maximum ZBC below 1, as shown in figures 1(c) and 2(d). The 60 ML film exhibits a similar feature (data not shown). However, in the case of the 165 ML film, there is a prominent peak at zero bias. We took many spectra in and outside different vortex

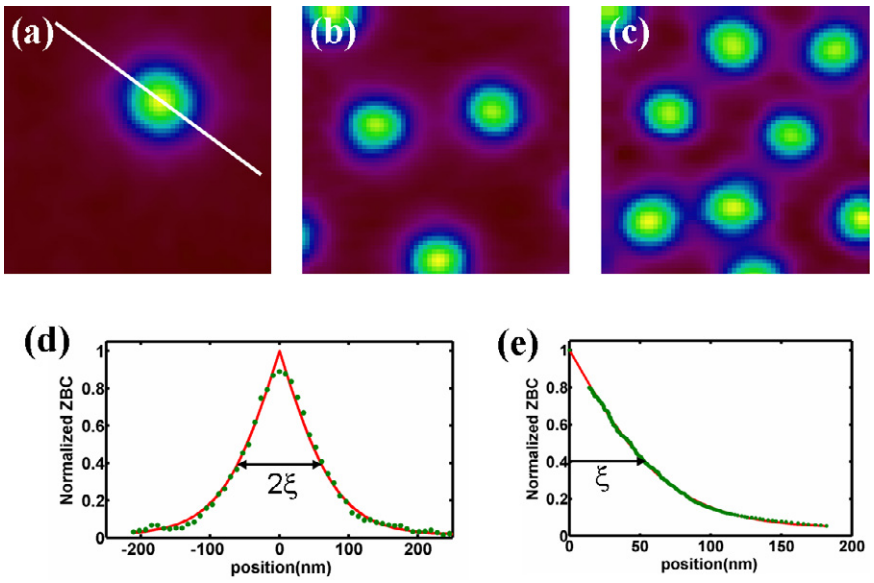

Figure 2. (a)–(c) A series of vortex images (468 nm × 468 nm) on a 25 ML Pb film obtained under different magnetic fields (37.5 G, 375 G and 750 G) at 2.25 K. (d) ZBC profile (green dots) along the white line in (a). The red solid curve is a theoretical fitting which gives a value of $\xi_{GL} = 59.6$ nm. (e) Reconstructed ZBC profile using a statistical method (see the text) and its best fitting curve.

cores, and this peak appeared reproducibly on all vortex cores. Consequently we believe that this ZBC peak at the vortex core is a real property of 165 ML film rather than an artefact of the measurement, although the ratio of the peak conductance to the high-bias (±12 meV) conductance is only 1.1 [4, 25].

The ZBCP reflects a much greater probability of finding the lowest-energy quasiparticle bound states at the Fermi energy at the vortex centre [22, 23]. In a thin film, scattering due to the interfacial disorder significantly reduces the electronic mean free path l, resulting in a pronounced mixing of the bound states and ultimately the disappearance of ZBCP. So the behaviour of ZBC suggests that the 165 ML Pb film is in the clean limit, while it is in the dirty limit [26] (i.e. $l \ll \xi_0$) when the thickness is smaller than 60 ML (1 ML corresponds to 0.286 nm).

We now focus on the quantitative analysis (see figure 1(d)). First, according to the BCS theory $\xi_0 = \hbar v_F/\pi\Delta(0)$ and $2\Delta(0)/k_B T_c = 4.38$, the BCS coherence length for thin film ξ_0^{film} can be calculated using $\xi_0^{film} T_c^{film} = \xi_0^{bulk} T_c^{bulk}$, where $T_c^{film}(d) = T_c^{bulk}(1 - d_c/d)$ [15]. Second, based on the vortex images for 25, 60 and 165 ML films, the Ginzburg–Landau (GL) coherence length ξ_{GL} can be obtained by the statistical method (explained in the next section). Then we get the electronic mean free path l using the relation $\xi_{GL}(T) = 0.85(\xi_0 l)^{1/2}(1 - T/T_c)^{-1/2}$ for a dirty limit sample [26]. On the other hand, the mean free path can be independently deduced from $l(d) \cong 2 \times d$ revealed by [15]. The results are shown in figure 1(d). The data clearly indicate that for the 160 ML film (47 nm) $l > \xi_0$, while $l \ll \xi_0$ for 15 ML (7.15 nm) and 60 nm (17.16 nm), which is consistent with the experiment.

The mean free path l is proportional to the normal state conductivity σ_n. For the ultrathin films, the dominant contribution to the resistivity is the scattering at the disordered interfacial layer. The resulting conductivity is roughly linearly dependent on thickness [15, 27]. With increasing thickness, the interface scattering becomes insignificant, and the conductivity will gradually deviate from linear behaviour and saturate at the bulk value. The behaviour of l in figure 1(d) agrees with this argument. As for ξ_{GL}, it is related to the upper critical field via the equation $H_{c2}(T) = \Phi_0/2\pi\xi_{GL}^2(T)$. $H_{c2}(T, d)$ increases when the film thickness decreases [26], and will be further modulated by quantum well states [13]. It is worth noting that the vortex size of the 60 ML film is significantly larger than the others in figure 1(d). Further experimental and theoretical efforts are needed to understand this interesting phenomenon.

3.2. Magnetic field dependence of the vortex core size

The field dependence of the vortex core size was previously studied on high-κ superconductors [28]. Pb film (9 ML) is known to have a low-κ value of 5 [15]. When a magnetic field is perpendicularly applied to the Pb film, a similar phenomenon occurs. Figures 2(a)–(c) display the vortices taken on a large terrace of a 25 ML Pb film under different magnetic fields at 2.25 K. It is clear that the size of the vortex core decreases with applied magnetic field from 37.5 to 750 G. The same tendency was also observed at 4.32 K (not shown).

In order to quantitatively analyse the experimental data, we attempt to determine the coherence length $\xi_{GL}(T, H)$, which is of the same order as the vortex core size. At low field (375 G), the intervortex distance (252 nm) is much larger than $\xi_0 = 83$ nm of the bulk Pb, so the vortices can be considered as isolated from each other. Based on the GL expression [26] for the superconducting order parameter $\psi(r)$ near the interface between a superconductor and a normal metal, the ZBC profile across an isolated vortex centre can be fitted using the following formula [7, 29]:

$$\sigma(r, 0) = \sigma_0 + (1 - \sigma_0) \times (1 - \tanh(r/(\sqrt{2}\xi))), \quad (1)$$

Table 1. Corresponding GL coherence lengths at different fields and different temperatures for a 25 ML Pb film calculated using the two methods mentioned in the text.

	4.32 K		2.25 K	
ξ_{GL} (nm)	Statistical	Average	Statistical	Average
37.5 G	73.2	80.4	51.3	59.3
75 G	72.7	77.9	48.0	55.5
375 G	—	—	—	46.9

where σ_0 is the normalized ZBC away from a vortex centre and r is the distance to the vortex core. A ZBC profile along the trace marked in figure 2(a) is shown in figure 2(d) as green dots, which clearly presents the spatial distribution of the density of states across a vortex core in a distance of ±200 nm. The fit, the red curve shown in figure 2(d), yields a coherence length $\xi_{GL} = 59.6$ nm at $T = 2.25$ K and $H = 37.5$ G. The results for 75 and 375 G are listed in table 1, which unequivocally reveals a decrease with increasing field.

It should be noted that the coherence lengths derived from the different profiles across the same vortex centre are not identical, which may be due to the anisotropic energy gap of Pb [30]. This determination gives a large uncertainty, especially at high temperatures. Consequently, the data shown in table 1 are the averaged results with large error bars. In order to eliminate the uncertainties, we try to use a statistical method to study the distribution of the ZBC values and to reconstruct the vortex profile [31]. Taking the vortex map in figure 2(a) as an example, which includes 64 × 64 ZBC pixel points on an area of 468 × 468 nm^2, we first count the number of points (N) larger than a specified ZBC value (σ_i), then calculate the corresponding distance to the vortex core r using $\pi r^2(\sigma_i)/468^2 = N(\sigma \geqslant \sigma_i)/64^2$. This expression is exact for a vortex profile with cylindrical symmetry [31]. The reconstructed data and a best fit curve are displayed in figure 2(e). It results in $\xi_{GL} = 51.0$ nm, slightly smaller than the former fitting value. However, as seen in table 1, the results derived from two methods for the vortices at different fields and temperatures indicate similar shrinking of the vortex core size with increasing field.

The magnetic behaviour has been investigated on a number of compound superconductors using muon spin rotation (μSR) [28]. A small-angle neutron-scattering (SANS) study on $CeCoIn_5$ [32] showed the same property. In spite of various physical characteristics, all tested materials have a large GL parameter κ. The theoretical calculations [33, 34] within the weak-coupling BCS theory for arbitrary T and H showed that the field dependence of the coherence length $\xi(H)$ can explain the magnetic properties extracted from μSR and SANS, i.e. $\xi(H) \sim 1/\sqrt{H}$ for larger fields. Using STS, we can directly detect the field dependent coherence length because STS measures the electronic density of states with atomic-scale spatial resolution instead of the magnetic flux density. Our study on Pb films reveals that for this elemental 2D superconductor with a small κ [15, 20], the GL coherence length also decreases with increasing magnetic field. It is obvious from table 1 that the quantitative value of $\xi(H)$ is not exactly proportional to $1/\sqrt{H}$, and the dependence becomes weaker at higher temperature. All the behaviours agree with the theory [33] that the H dependency of ξ is weakened by scattering and temperature, and disappears in the dirty limit and as $T \to T_c$.

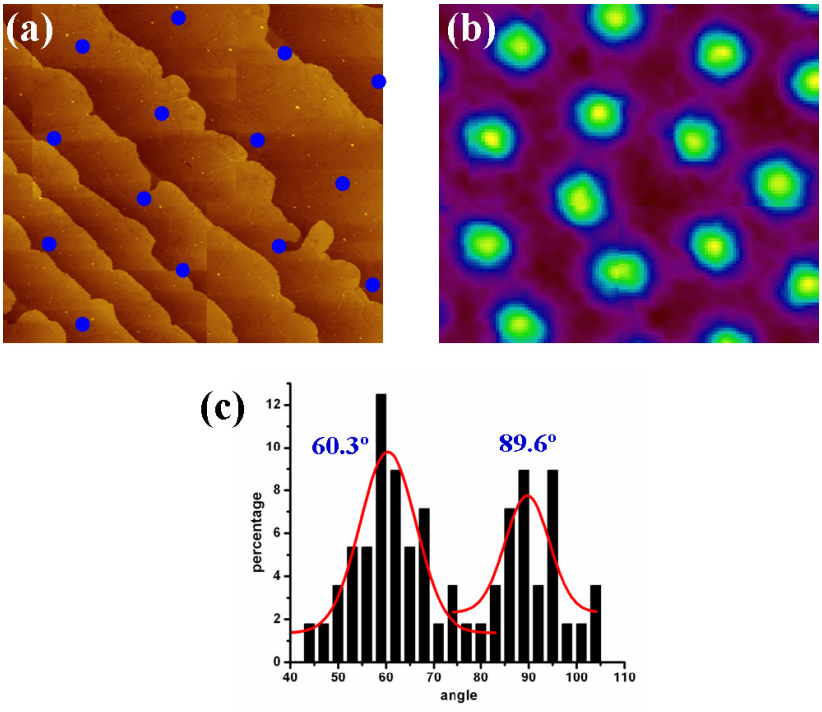

Figure 3. (a) A mosaic STM image (930 nm × 830 nm). (b) The vortex image of the same area shown in (a). The blue dots in (a) indicate the centres of the vortex in (b). The magnetic field is 375 G and the temperature is 4.32 K. (c) The corresponding distribution of angles formed by three neighbouring vortices and the Gaussian fit (red curve) show two preferred angles of 60.3° and 89.6°.

3.3. Vortex spatial distribution

In the presence of high field, vortices will arrange in the form of a hexagonal structure in a defect-free type-II superconductor. However, in our case a distorted hexagonal lattice was observed, independent of film thickness, temperature or applied field, as shown in figures 2(b) and (c) and a mosaic vortex image in figure 3(b). Figure 3(a) displays the spatial distribution of vortices on the corresponding topographic image. It can be seen that the step edges do not show preference in pinning the vortex. The vortex spacing $d = 250.3 \pm 35.9$ nm at 375 G, is consistent with the theoretical value (252.5 nm) using $d = (2\Phi_0/\sqrt{3}H)^{1/2}$. Measuring the triangle formed by three neighbouring vortices, we obtain the angle distribution of the triangles. The result is shown in figure 3(c). By Gaussian fitting, two preferred angles of 60.3° and 89.6°, corresponding to a hexagonal lattice and a square one, respectively, can be obtained. Such a vortex distribution can be ascribed to the pinning by some surface defects such as stacking faults or grain boundaries. Moreover, the local defects on the 2D vortex lattice are also related to the measuring temperature or applied field [9, 10]. The fact that the vortices will rearrange under a new magnetic field indicates that the surface pinning is not very strong.

4. Summary

The vortex properties of atomically flat Pb films have been studied by low temperature STM/STS. We investigate the transition from the clean limit to the dirty limit with decreasing thickness, and reveal the decrease of the vortex core size with increasing magnetic field. While the behaviours in previous experimental and theoretical studies have usually been characterized on the compound superconductors, the work presented here is valuable for understanding the vortex properties at reduced dimensionality.

Acknowledgments

This work was financially supported by the National Natural Science Foundation and the Ministry of Science and Technology of China.

References

[1] Abrikosov A A 1957 *Sov. Phys.—JETP* **5** 1174
[2] Cribier D, Jacrot B, Rao L M and Farnoux B 1964 *Phys. Lett.* **9** 106
[3] Essmann U and Trauble H 1967 *Phys. Lett.* A **24** 526
[4] Hess H F, Robinson R B, Dynes R C, Valles J M and Waszczak J V 1989 *Phys. Rev. Lett.* **62** 214
[5] Oral A, Bending S J and Henini M 1996 *Appl. Phys. Lett.* **69** 1324
[6] Renner C, Kent A D, Niedermann P, Fischer Ø and Lévy F 1991 *Phys. Rev. Lett.* **67** 1650
[7] Eskildsen M R, Kugler M, Tanaka S, Jun J, Kazakov S M, Karpinski J and Fischer Ø 2002 *Phys. Rev. Lett.* **89** 187003
[8] Pan S H, Hudson E W, Gupta A K, Ng K W, Eisaki H, Uchida S and Davis J C 2000 *Phys. Rev. Lett.* **85** 1536
[9] van Baarle G J C, Troianovski A M, Nishizaki T, Kes P H and Aarts J 2003 *Appl. Phys. Lett.* **82** 1081
[10] Guillamon I, Suderow H, Fernandez-Pacheco A, Sese J, Cordoba R, De Teresa J M, Ibarra M R and Vieira S 2009 *Nat. Phys.* **5** 651
[11] Fischer Ø, Kugler M, Maggio-Aprile I, Berthod C and Renner C 2007 *Rev. Mod. Phys.* **79** 353
[12] Guo Y *et al* 2004 *Science* **306** 1915
[13] Bao X-Y, Zhang Y-F, Wang Y, Jia J-F, Xue Q-K, Xie X C and Zhao Z-X 2005 *Phys. Rev. Lett.* **95** 247005
[14] Özer M M, Thompson J R and Weitering H H 2006 *Nat. Phys.* **2** 173
[15] Özer M M, Thompson J R and Weitering H H 2006 *Phys. Rev.* B **74** 235427
[16] Dolan G J and Silox J 1973 *Phys. Rev. Lett.* **30** 603
[17] Hasegawa S, Matsuda T, Endo J, Osakabe N, Igarashi M, Kobayashi T, Naito M, Tonomura A and Aoki R 1991 *Phys. Rev.* B **43** 7631
[18] Nishio T *et al* 2008 *Phys. Rev. Lett.* **101** 167001
[19] Cren T, Fokin D, Debontridder F, Dubost V and Roditchev D 2009 *Phys. Rev. Lett.* **102** 127005
[20] Ning Y X, Song C L, Guan Z L, Ma X C, Chen X, Jia J F and Xue Q K 2009 *Europhys. Lett.* **85** 27004
[21] Li J L *et al* 2002 *Phys. Rev. Lett.* **88** 066101
[22] Shore J D, Huang M, Dorsey A T and Sethna J P 1989 *Phys. Rev. Lett.* **62** 3089
[23] Gygi F and Schlüter M 1991 *Phys. Rev.* B **43** 7609
[24] Wang K, Zhang X, Loy M M T, Chiang T C and Xiao X 2009 *Phys. Rev. Lett.* **102** 076801
[25] Guillamon I, Suderow H, Vieira S, Cario L, Diener P and Rodiere P 2008 *Phys. Rev. Lett.* **101** 166407
[26] Tinkham M 1996 *Introduction to Superconductivity* 2nd edn (New York: McGraw-Hill)
[27] Vilfan I, Henzler M, Pfennigstorf O and Pfnür H 2002 *Phys. Rev.* B **66** 241306
[28] Sonier J E 2004 *J. Phys.: Condens. Matter* **16** S4499
[29] Bergeal N *et al* 2006 *Phys. Rev. Lett.* **97** 077003
[30] Rochlin G I 1967 *Phys. Rev.* **153** 513
[31] Kohen A *et al* 2005 *Appl. Phys. Lett.* **86** 212503
[32] DeBeer-Schmitt L, Dewhurst C D, Hoogenboom B W, Petrovic C and Eskildsen M R 2006 *Phys. Rev. Lett.* **97** 127001
[33] Kogan V G and Zhelezina N V 2005 *Phys. Rev.* B **71** 134505
[34] Kogan V G, Prozorov R, Bud'ko S L, Canfield P C, Thompson J R, Karpinski J, Zhigadlo N D and Miranović P 2006 *Phys. Rev.* B **74** 184521